

Giant temperature dependence of the spin reversal field in magnetoelectric chromia

Lorenzo Fallarino, Andreas Berger, and Christian Binek

Citation: [Applied Physics Letters](#) **104**, 022403 (2014); doi: 10.1063/1.4861780

View online: <http://dx.doi.org/10.1063/1.4861780>

View Table of Contents: <http://scitation.aip.org/content/aip/journal/apl/104/2?ver=pdfcov>

Published by the [AIP Publishing](#)



Re-register for Table of Content Alerts

Create a profile.



Sign up today!



Giant temperature dependence of the spin reversal field in magnetoelectric chromia

Lorenzo Fallarino,¹ Andreas Berger,¹ and Christian Binek^{1,2,a)}

¹*CIC Nanogune Consolider, Tolosa Hiribidea 76, 20018 Donostia-San Sebastian, Spain*

²*IKERBASQUE, Basque Foundation for Science, 48011 Bilbao, Spain*

(Received 16 September 2013; accepted 28 December 2013; published online 13 January 2014)

Magnetic field-induced reversal of surface spin polarization for the magnetoelectric antiferromagnet chromia is studied via magnetometry in (0001)-textured thin films of various thicknesses. Reversal solely by magnetic means has been experimentally evidenced in sufficiently thin films. It sets the field-response of chromia films apart from bulk behavior, where switching between time-reversed single domain states requires the simultaneous presence of electric and magnetic fields. In our detailed experiments, we furthermore observe a giant sensitivity of the coercive field on temperature, thus, indicating the potential of magnetoelectric antiferromagnets as promising candidates for energy assisted magnetic recording media. © 2014 AIP Publishing LLC. [<http://dx.doi.org/10.1063/1.4861780>]

The antiferromagnetic (AFM) insulator α -Cr₂O₃ (chromia) is an archetypical magnetoelectric (ME) material. In magnetoelectrics, an applied electric field, E , can induce magnetization and conversely an applied magnetic field, H , can induce electric polarization.^{1,2} Recently, strong interest in ME antiferromagnets revived, which was fueled by their potential for ultra-low power dissipation spintronic devices.^{3,4} A series of breakthroughs in the widely studied oxide α -Cr₂O₃ helped overcoming the fundamental problem that spin-orbit coupling and thus, the linear ME effect are small. Key experiments utilized the exchange bias effect in heterostructures, in which a ferromagnetic thin film was coupled via the quantum mechanical exchange interaction to an adjacent chromia pinning layer.^{5,6} In particular, the pioneering experiment reported in Ref. 5 explored the effect that ME annealing has onto the sign of the exchange bias field. ME annealing is a protocol whereby the exchange bias system is cooled to below chromia's Néel temperature, T_N , in the simultaneous presence of E and H .⁷ ME annealing provides control over the sign of the exchange bias field, i.e., the sign of the shift of the hysteresis loop along the magnetic field axis, through experimental control over the sign of the field product EH .⁵ Later, isothermal switching of the exchange bias field was demonstrated exploiting magnetoelectricity in the nonlinear regime.⁶ Here, a field-product above a critical threshold $(EH)_c$ switches the sign of the exchange bias field.

The physical mechanism of the voltage-controlled exchange bias effect is based on the phenomenon of boundary magnetization (BM) emerging at the surface or interface of a ME antiferromagnet. The peculiar symmetry of ME antiferromagnets, in general, and chromia, in particular, gives rise to a spin-polarized surface or BM if the antiferromagnet is in one of its two degenerate 180° domain state.^{8,9} BM is a symmetry enabled equilibrium property and therefore robust against the potential presence of surface

roughness. This property is theoretically and experimentally well-established.^{6,8–10} It is in sharp contrast to surface magnetic states of conventional antiferromagnets such as Cr where step-terraces at the (001) surface create alternating local magnetization and, hence, vanishing net surface polarization.¹¹

The inset of Fig. 1 shows a cartoon highlighting the major qualitative properties of the AFM spin structure of c -oriented chromia with BM at its (0001) surface. The surface layer of Cr³⁺ moments shows uniformly aligned spins constituting the BM. For simplicity an ideal surface is depicted. Note that stepped surfaces remain spin-polarized as long as the underlying AFM spin structure is single domain.⁶ The cartoon of Fig. 1 indicates the AFM single domain state via two representative layers of Cr³⁺ moments below the surface. As an example, the case of a positive AFM order parameter and positive BM is depicted. The degenerate time reversed spin structure with negative AFM order parameter has the corresponding negative BM. Exchange coupling links the BM intimately with the bulk AFM spin structure. Up to now, switching of BM has only been documented in the presence of electric fields. This holds for isothermal switching via the critical field product $(EH)_c$ and for the thermally assisted selection of the orientation of the BM via ME annealing in the simultaneous presence of E and H on cooling.

In this Letter we show that, in the case of chromia (0001) thin films, a moderate magnetic field can suffice to select and switch between the AFM single domain states and their corresponding BM. This reversal of the BM and the simultaneous reversal of the underlying AFM spin structure by pure magnetic means becomes possible because the Zeeman energy of the surface spins make a sizable contribution to the total magnetic energy in ME thin film. In the bulk, magnetic surface energies contribute only marginally to the total magnetic energy. Therefore, a potential reversal of the BM leaves the bulk AFM spin structure virtually unaffected. This, in turn, implies that a field-induced reversal of the BM is not stabilized in zero field by the AFM spin structure in bulk

^{a)}On sabbatical leave from Department of Physics and Astronomy and the Nebraska Center for Materials and Nanoscience, University of Nebraska, Lincoln, Nebraska 68588-0111, USA.

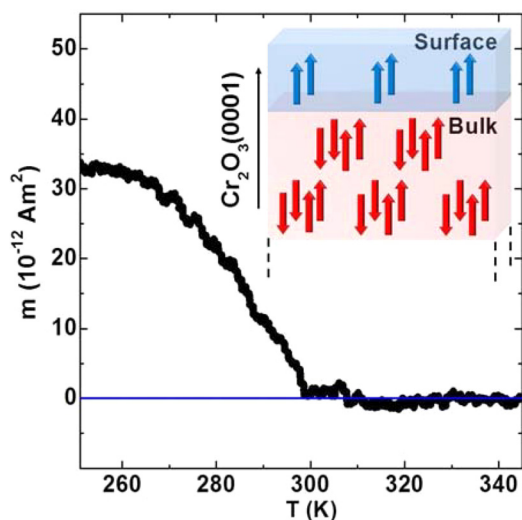


FIG. 1. Field cooling m vs. T data for sample 1 measured in a magnetic field of 10 mT applied normal to the film.¹⁷ The horizontal line is the zero-level after linear background subtraction resulting in $m = 0$ for $T > T_N$. The inset shows a schematic of the sample spin structure at $T < T_N$ in an AFM single domain state (lower two layers of arrows represent AFM structure of Cr^{3+} spins in the bulk), which is accompanied by a positive boundary magnetization (top layer representing the surface).

type samples. In addition to pure magnetic field switching, our magnetometric investigations of thin film samples furthermore show that the specific spin reversal field, which switches between up and down BM, hereafter called the coercive field H_c , depends extremely sensitive on temperature and film thickness. This dependence can be quantified by the parameter¹² $|\partial\mu_0 H_c / \partial T|$ which, to the best of our knowledge, is at least an order of magnitude larger than any prior observation. Together with material properties, such as thermal conductivity and grain size, it constitutes the figure of merit of magnetic media for the emerging technology of heat assisted magnetic recording (HAMR).¹³

Cr_2O_3 thin films of $d = 26, 50,$ and 60 nm thickness subsequently labeled samples 1, 2, and 3 were deposited on Al_2O_3 (0001) substrates by RF magnetron sputtering from a Cr_2O_3 target. Before deposition, the substrates were ultrasonically cleaned using acetone, methanol, and deionized water in consecutive cleaning steps. Samples were grown at room temperature by RF-sputtering at 200 W power in an Ar gas atmosphere of 3.9×10^{-1} Pa. XRD θ - 2θ (PANalytical X'Pert Pro with Cu $K\alpha$ radiation) patterns of all three as-prepared samples show a broad peak at $2\theta = 37.9^\circ$ with a FWHM of 5.2° , characteristic for the orthorhombic CrO_3 phase with (112) orientation. Post deposition, the films were thermally annealed at 1000°C in vacuum (3 Pa) for 1 h. Thermal annealing transformed this initial phase into (0001) oriented Cr_2O_3 (chromia) characterized by a peak at $2\theta = 39.75^\circ$ (0006) with a FWHM of 0.57° (sample 1), 0.54° (sample 2), 0.43° (sample 3) and one at $2\theta = 85.7^\circ$ (00012).¹⁴

XRD Φ -scans of the (10–14) reflection revealed the formation of twin domains, which is known to accompany the thermal annealing.¹⁵ It is the (0001) surface layer of the Cr_2O_3 films, that is Cr terminated and has its surface spin alignment rigidly coupled to the AFM spin structure of the film, thus originating the BM.⁶ Due to the twin domains, a different magnetic sublattice appears at the (0001) surface

and thus, the BM depends on the ratio of the twin domains.¹⁶ Magnetic measurements have been performed using a commercial Quantum Design SQUID-VSM magnetometer, equipped with Evercool closed cycle refrigeration.

Fig. 1 shows the temperature dependence of the out-of-plane magnetic moment, m , of the sample 1 upon field-cooling (FC) in an applied axial magnetic field of $\mu_0 H = 0.01$ T.¹⁷ A field of 0.01 T suffices to saturate the BM while keeping perturbations of the AFM order at a minimum. This has been concluded from zero field-heating (ZFH) measurements (not shown) obtained after FC in an axial magnetic fields of increasing strength. Note that the BM is also measured as remnant magnetic moment on ZFH, which implies that FC in positive H selects an AFM single domain state with positive AFM order parameter (see inset Fig. 1). The AFM spin structure and its corresponding BM have been energetically favored by the Zeeman energy via the magnetic field-induced alignment of the surface spins. The growth kinetics of the spin structure of the film is determined by the surface. Here, due to reduced interaction neighbors, spins are aligned preferentially parallel to the applied field and act as a two dimensional defect before AFM long range order is fully established. Condensation of the AFM order evolves from the surface with preferential single domain growth in successive layers due to strong coupling between the BM and the AFM order parameter. The smallness of the Zeeman energy of the BM in an applied field renders this mechanism ineffective if the ratio of surface-to-bulk spins becomes small in the limit of bulk chromia. We find that the pure magnetic FC remains an efficient selection mechanism of a particular domain in chromia thin films up to about 60 nm thickness even though rapidly increasing magnetic fields are required with increasing film thickness.

All our thin films show reduced Néel temperatures relative to the bulk critical temperature $T_N^{\text{bulk}} = 307$ K. Such a thickness dependence of the critical temperature is well-known from the literature, and it is important to note that in the regime $26 \leq d \leq 60$ nm this reduction is not the result of finite-size scaling but rather defect induced.¹⁸ The critical temperatures of our sputtered thin films $T_N \approx 297$ K ($d = 26$ nm), 299 K ($d = 50$ nm), and 300 K ($d = 60$ nm) are remarkably close to $T_N^{\text{bulk}} = 307$ K in comparison with thin film critical temperatures reported in the literature, indicating excellent sample quality.¹⁸

Figs. 2(b) and 2(c) shows the experimental protocol, which allows to reverse the BM and the AFM order parameter by pure magnetic means. Conceptually, reversal of BM is most clearly measured via an isothermal m vs. H hysteresis. However, in the case of our AFM thin films, magnetometry in large applied magnetic fields is plagued by an ill-defined background signal which masks the low moment of the BM. Therefore, we conducted the more elaborate T - and H -dependent protocol visualized in Figs. 2(b) and 2(c). For each sample, this protocol allows to determine the T -dependence of the specific magnetic field where reversal of the BM sets in.

In an initializing step, we cooled the sample from $T = 350$ K to $T = 100$ K in a positive magnetic field (0.01 T for sample 1, see $\mu_0 H$ vs. time protocol in Fig. 2(c)) to polarize the surface spins and thus establishing the AFM single

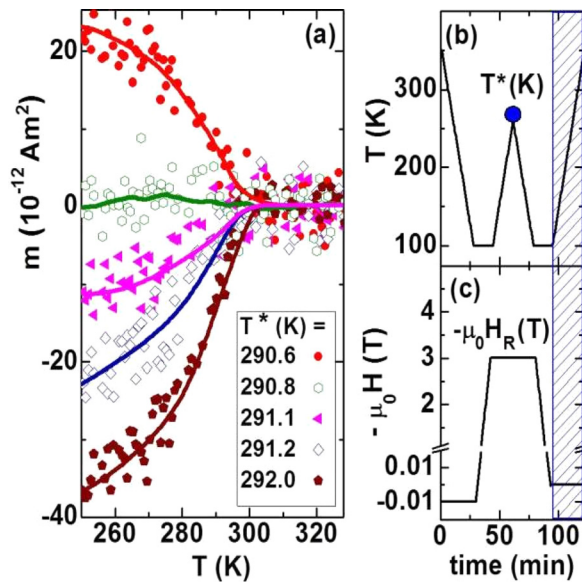


FIG. 2. (a) ZFH m vs. T data of sample 1 after applying the field-temperature sequence shown in (b) and (c) with $\mu_0 H_R = -3 \text{ T}$ and temperatures $T^* = 290.6$ (circles), 290.8 (open-hexagons), 291.1 (triangle), 291.2 (open-rhombi), and 292.0 K (pentagons). The solid lines are guides to the eye. A linear background has been subtracted from the data sets. (b) and (c) experimental protocol showing temperature variation vs. time (b) and the simultaneous magnetic field variation vs. time (c) for one particular example of T^* and reversal field $\mu_0 H_R$. The dashed rectangular regions indicate the ZFH part of the sequence, where the data in (a) were measured.

domain state. The FC procedure is followed by applying the reversal magnetic field, $\mu_0 H_R$ at $T = 100 \text{ K}$ and FH to a variable target temperature T^* . Here, the system is maintained in thermal equilibrium for a waiting time of 2 min. After the sample has been equilibrated at T^* , it is field-cooled again in the presence of the $\mu_0 H_R$ down to $T = 100 \text{ K}$. Note that T^* does not exceed the magnetic ordering temperature, and neither does the protocol allow for the sample temperature to overshoot upon approaching T^* . The protocol ensures that AFM long-range order is maintained at all times without crossover into the paramagnetic phase. After FC from T^* back to 100 K, a ZFH curve has been measured to study the temperature dependence of the remnant BM. Note that true ZFH conditions have been achieved by quenching the superconducting magnet to eliminate any non-hysteretic magnetic background contribution. Some details of the experimental protocol outlined above are particularly crucial for the consistent interpretation of our data. It is of paramount importance to keep in mind that the data displayed in Fig. 2(a) are ZFH data and that the applied reversal fields of substantial magnitude have negative sign, while the remnant moment of the sample has positive sign until reversal through thermal activation is achieved. These facts eliminate the possibility that the measured moments are field-induced residuals of finite susceptibility or the result of long-range ordered FM impurities. Fig. 2(a) shows selected ZFH curves for $T^* = 290.6$ (circles), 290.8 (open-hexagons), 291.1 (triangle), 291.2 (open-rhombi), and 292.0 K (pentagons), respectively, after having previously applied a reversal field of $\mu_0 H_R = -3 \text{ T}$. As one can clearly see from these data sets, the temperature dependent magnetic switching of the BM takes place in a small temperature range around $T_F = 291 \text{ K}$. At $T \ll T_F$, the single domain state and its accompanying

positive BM are virtually unperturbed by the presence of the negative reversal field. However, upon approaching and ultimately exceeding $T_F = 291 \text{ K}$ the BM and with it the AFM single domain state are reversed. This takes place because the Zeeman energy of the BM and its coupling to the AFM order parameter lifts the degeneracy of the two AFM single domain states. At T^* thermal excitations reduce the free energy barrier separating the two AFM domain states. Thus, upon reaching a sufficiently high T^* , the applied reversal field switches the entire film into the energetically favored spin structure, which becomes a stable degenerate state in zero field.

Fig. 3 shows the result of numerical integration

$$\langle m \rangle_T = \frac{1}{50 \text{ K}} \int_{250 \text{ K}}^{300 \text{ K}} m(T) dT, \quad (1)$$

of the ZFH data m vs. T of sample 1 for different reversal magnetic field values $\mu_0 H_R = -7 \text{ T}$ (circles), -5 T (squares), and -3 T (triangles), respectively. Vertical bars represent the average standard deviations of the m -data for $250 \leq T \leq 300 \text{ K}$. The dependence of $\langle m \rangle_T$ on T^* is used to define the flipping temperature $T_F(\mu_0 H_R, d)$. In the hypothetical absence of noise, magnetization reversal of the BM could be deduced from a single data point m . However, in order to take advantage of statistics, the average defined via Eq. (1) has been introduced. Although the integration interval has an element of arbitrariness the results of our analysis do not depend on details of the definition of $\langle m \rangle_T$. The $\langle m \rangle_T$ vs. T^* data illustrate that switching between the two AFM + BM domains of Cr_2O_3 takes place at a reverse field dependent $T^* = T_F$, where T_F is defined by the inflection point of $\langle m \rangle_T$ vs. T^* indicated by dashed horizontal lines in Figures 3(a)–3(c). The applied reversal field favors reduction and ultimately reversal of $\langle m \rangle_T$ while the bulk AFM order stabilizes its initial orientation. In successive measurements, the reversal field is applied at ever increasing temperature T^* . With increasing T^* the stabilizing effect of the AFM order parameter decreases and $\langle m \rangle_T$ ultimately reverses at $T^* = T_F$.

The center panel of Fig. 3 depicts the cartoon with positive BM and positive AFM order parameter on the left and the switched state on the right. The data sets in Fig. 3 show that $T_F(\mu_0 H_R = \mu_0 H_c, d)$ increases with decreasing absolute value of the coercive field $\mu_0 H_c$. Also, it is worth to mention that with increasing T_F the transition from positive to negative BM becomes increasingly sharp.

Fig. 4 represents a summary of our extensive magnetometric investigations and allows deducing their relevance for application in potential future magnetic recording media. Triangles, squares, and circles show $-\mu_0 H_c$ vs. T_F for samples 1, 2, and 3, respectively. Horizontal bars quantify the transition width of the reversal of the BM determined from the full width at half maximum of $\frac{d\langle m \rangle_T}{dT^*}$. Extrapolation of $-\mu_0 H_c$ vs. T_F towards the interception with the T axis defines $T_F(\mu_0 H_c = 0, d)$. At this temperature an infinitesimal small magnetic field suffices to reverse the BM. Although BM and AFM order parameter are substantially reduced in magnitude due to thermal excitation they both remain finite at $T_F(\mu_0 H_c = 0, d)$. Breaking of the AFM order requires $T \geq T_N$. $T_F(\mu_0 H_c = 0, d)$ increases with increasing thickness of the Cr_2O_3 layer and is expected to approach asymptotically the bulk Néel temperature. In addition, the steepness of

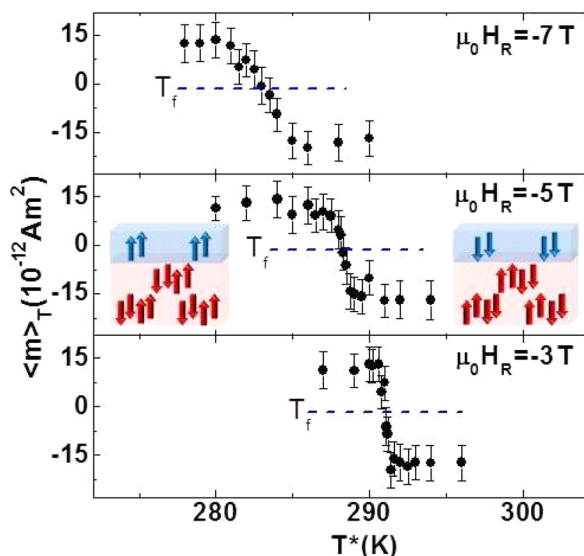


FIG. 3. Numerical integral $\langle m \rangle_T$ calculated from ZFH curves m vs. T for $250 < T < 300$ K and plotted vs. T^* for three different reversal fields $\mu_0 H_R = -3$ T (triangle), -5 T (squares), and -7 T (circles). The dashed lines indicate the respective T_F defined as inflection point of $\langle m \rangle_T$ vs. T^* . The two insets show schematics of the two AFM single domain states with corresponding surface magnetization of opposite sign.

$-\mu_0 H_c$ vs. T_F increases with increasing film thickness. This is quantified by the thickness dependence of $|\mu_0 \frac{dH_c}{dT_F}| \approx 1.10$ T/K (60 nm), 0.78 T/K (50 nm), and 0.56 T/K (26 nm). Comparison of $|\mu_0 \frac{dH_c}{dT_F}|$ for chromia thin films with presently investigated magnetic media materials that are optimized for energy assisted magnetic recording reveals the enormous potential of magnetoelectric antiferromagnets with switchable BM for magnetic recording media, because values of only up to 0.09 T/K, i.e., one order of magnitude smaller than measured here, have been reported so far.¹² Also the fact that it is the ferromagnetic surface layer that responds to the externally applied field, makes these materials especially suitable for utilization in magnetic recording schemes, as this would allow for an ideal minimization of the effective head-media spacing. In order to develop chromia thin films into practical heat assisted recording media, tuning of the Néel temperature towards higher ordering temperatures is a necessary prerequisite. Currently, there are multiple pathways being explored to achieve this goal, which include straining and doping chromia films.^{19,20}

In conclusion, we have shown that the magnetoelectric antiferromagnet chromia shows a hitherto unreported effect when geometrically confined in the form of a thin film. Surface spin polarization, which is a generic property of magnetoelectric antiferromagnets in a single domain state, can be reversed solely by magnetic means. This finding is in strong contrast to bulk chromia where, in the generally accepted picture of boundary magnetization, a simultaneous presence of electric and magnetic fields is necessary to achieve reversal of the surface magnetization and the underlying AFM spin structure. The coercive fields of the chromia thin films show a giant temperature sensitivity. It is an at least ten-fold increase over the temperature dependent change in coercivity known from materials currently investigated as media for energy assisted magnetic recording. This property of chromia thin films suggests magnetoelectric antiferromagnets as promising

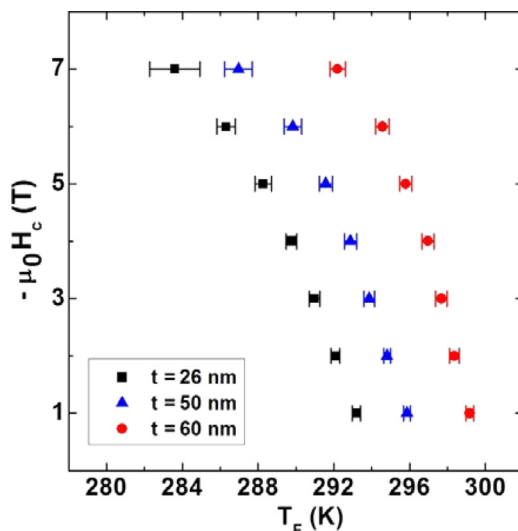


FIG. 4. Coercive field, $-\mu_0 H_c$, versus T_F for sample 1 of 26 nm (squares), sample 2 of 50 nm (triangles), and sample 3 of 60 nm thickness (circles). Horizontal bars quantify the transition width of reversal determined from the full width at half maximum of $d\langle m \rangle_T/dT^*$.

candidates for HAMR by means of storing magnetic bits via the surface magnetization of otherwise antiferromagnetically ordered films.

We acknowledge funding from the Basque Government under Program No. PI2012-47 and the Spanish Ministry of Economy and Competitiveness under Project No. MAT2012-36844. Ch. Binek gratefully acknowledges support by the Basque Foundation for Science, Ikerbasque, by NSF through MRSEC DMR 0213808, by the NRC/NRI supplement to MRSEC, and by STARnet, a Semiconductor Research Corporation program.

- ¹D. N. Astrov, Sov. Phys. JETP **11**, 708 (1960) [Zh. Eksp. Teor. Fiz. **38**, 984-985 (1960) (in Russian)].
- ²T. H. O'Dell, *The Electrodynamics of Magneto-Electric Media* (North-Holland, 1970).
- ³Ch. Binek and B. Doudin, *J. Phys.: Condens. Matter* **17**, L39 (2005).
- ⁴M. Fiebig, *J. Phys. D: Appl. Phys.* **38**, R123 (2005).
- ⁵P. Borisov, A. Hochstrat, X. Chen, W. Kleemann, and C. Binek, *Phys. Rev. Lett.* **94**, 117203 (2005).
- ⁶X. He, Y. Wang, N. Wu, A. N. Caruso, E. Vescovo, K. D. Belashchenko, P. A. Dowben, and C. Binek, *Nat. Mater.* **9**, 579 (2010).
- ⁷T. J. Martin and J. C. Anderson, *IEEE Trans. Magn.* **2**, 446 (1966).
- ⁸K. D. Belashchenko, *Phys. Rev. Lett.* **105**, 147204 (2010).
- ⁹A. F. Andreev, *JETP Lett.* **63**, 758 (1996).
- ¹⁰N. Wu, X. He, A. L. Wysocki, U. Lanke, T. Komesu, K. D. Belashchenko, C. Binek, and P. A. Dowben, *Phys. Rev. Lett.* **106**, 087202 (2011).
- ¹¹R. Wiesendanger, H. J. Güntherodt, G. Güntherodt, R. J. Gambino, and R. Ruf, *Phys. Rev. Lett.* **65**, 247 (1990).
- ¹²J. U. Thiele, K. R. Coffey, M. F. Toney, J. A. Hedstrom, and A. J. Kellock, *J. Appl. Phys.* **91**, 6595 (2002).
- ¹³J. U. Thiele, S. Maat, and E. E. Fullerton, *Appl. Phys. Lett.* **82**, 2859 (2003).
- ¹⁴S. Y. Jeng, J. B. Lee, H. Na, and T. Y. Seong, *Thin Solid Films* **518**, 4813 (2010).
- ¹⁵J. Wang, A. Gupta, and T. M. Klein, *Thin Solid Films* **516**, 7366 (2008).
- ¹⁶N. Iwata, T. Kuroda, and H. Yamamoto, *Jpn. J. Appl. Phys., Part 1* **51**, 11PG12 (2012).
- ¹⁷To improve the signal to noise ratio the displayed data represent the arithmetic average of six independent data sets. A linear background has been determined for $T > 305$ K $> T_N$ ($d = 26$ nm) and after extrapolation to $T < T_N$ removed from the data.
- ¹⁸X. He, W. Echtenkamp, and C. Binek, *Ferroelectrics* **426**, 81 (2012).
- ¹⁹Y. Kota, H. Imamura, and M. Sasaki, *Appl. Phys. Express* **6**, 113007 (2013).
- ²⁰S. Mu, A. L. Wysocki, and K. D. Belashchenko, *Phys. Rev. B* **87**, 054435 (2013).